Sains Malaysiana 45(2)(2016): 289–296

Free Convection Boundary Layer Flow on a Horizontal Circular Cylinder in a Nanofluid with Viscous Dissipation

(Olakan Bebas Aliran Lapisan Sempadan pada Silinder Bulat Mengufuk dalam Nanobendalir dengan Pelesapan Likat)

MUHAMMAD KHAIRUL ANUAR MOHAMED, NOR AIDA ZURAIMI MD NOAR, MOHD ZUKI SALLEH* & ANUAR ISHAK

ABSTRACT

In this paper, the problem of free convection boundary layer flow on a horizontal circular cylinder in a nanofluid with viscous dissipation and constant wall temperature is investigated. The transformed boundary layer equations are solved numerically using finite difference scheme namely the Keller-box method. Numerical solutions were obtained for the reduced skin friction coefficient, Nusselt number and Sherwood number as well as the velocity and temperature profiles. The features of the flow and heat transfer characteristics for various values of the Brownian motion parameter, thermophoresis parameter, Lewis number and Eckert number were analyzed and discussed.

Keywords: Free convection; horizontal circular cylinder; nanofluid; viscous dissipation

ABSTRAK

Dalam kajian ini, masalah olakan bebas aliran lapisan sempadan pada silinder bulat mengufuk dalam nanobendalir dengan pelesapan likat dan suhu permukaan malar dikaji. Persamaan lapisan sempadan terjelma diselesaikan secara berangka dengan menggunakan skim beza terhingga dikenali sebagai kaedah kotak Keller. Penyelesaian berangka diperoleh bagi pekali geseran kulit diturunkan, nombor Nusselt dan nombor Sherwood diturunkan serta profil halaju dan suhu. Ciri aliran dan pemindahan haba bagi pelbagai nilai parameter gerakan Brown, parameter termoforesis, nombor Lewis dan nombor Eckert dianalisis dan dibincangkan.

Kata kunci: Nanobendalir; olakan bebas; pelesapan likat; silinder bulat mengufuk

INTRODUCTION

In recent years, many investigations have been made on the flow of a nanofluid in a convective boundary layer past various types of surface such as stagnation point, stretching sheet, horizontal circular cylinder as well as a solid sphere. This type of fluid is believed can enhanced thermal conductivity, viscosity, thermal diffusivity and convective heat transfer compared to those base fluids like water and oil. This has made nanofluids employed in plenty of important applications which involves fluid as cooling medium in industrial outputs for example act as smart fluid in battery devices, as nanofluid coolant in car radiator, brake fluid, fuel catalyst to improve engine combustion and also act to cooling microchip in electronic devices (Wong & De Leon 2010). Based on the large contributions and issues, this topic has attracted many researchers to study and expand this knowledge for example from the works by Arifin et al. (2011), Bachok et al. (2010), Kakaç and Pramuanjaroenkij (2009), Khan and Pop (2010), Nazar et al. (2011), Tiwari and Das (2007), Yacob et al. (2011), Tham and Nazar (2012) and recently by Anwar et al. (2013), Roşca and Pop (2014), Tham et al. (2014) and Yusoff et al. (2014).

The study of boundary layer flow on a horizontal circular cylinder was first studied by Blasius (1908). Blasius (1908) successfully solved the momentum equation of forced convection boundary layer flow. The energy equation for this problem was then solved by Fr¨ossling (1958) with considering the constant wall temperature (CWT). Since then, this topic has attracted many researchers to study the constant wall temperature and constant heat flux. Merkin (1977, 1976) considered the free and mixed convection boundary layer on an isothermal horizontal cylinder with CWT and became the first who obtained the exact solution for this problem. Merkin and Pop (1988) updated this topic with constant heat flux. Next, Nazar et al. (2002) extended the work by Merkin (1976) and Merkin and Pop (1988) to a micropolar fluid. Molla et al. (2006) investigated the heat generation effects on free convection flow on an isothermal horizontal circular cylinder before Tahavvor and Yaghoubi (2010) done the experimental and numerical study of frost formation on a free convection over a cold horizontal circular cylinder. Salleh and Nazar (2010) extended Nazar et al. (2002) work with Newtonian heating. Recently, Rosca et al. (2014) studied the mixed convection boundary layer flow close to the lower stagnation point of a horizontal circular cylinder. The stability analysis for dual solution is discussed and it is concluded that the upper branch solutions are stable and physically realizable, while the lower branch solutions

are unstable. Singh and Makinde (2014) observed axis symmetric slip flow on a vertical cylinder while Sarif et al. (2014) updated Nazar et al. (2002) and Salleh and Nazar (2010) works with convective boundary conditions. These three problems were successfully solved numerically using the Keller-box method.

It is known that the viscous dissipation or internal friction is the rate of the work done againts viscous forces which is irreversibly converted into internal energy. The effect of viscous dissipation is significant especially for high velocity flow, highly viscous flow with moderate velocity and for fluid with moderate Prandtl number and velocities. Hence, viscous dissipations effect is important to study in order to understand the behavior of temperature distributions when the internal friction cannot be neglected. Gebhart (1962) is the first person who studied viscous dissipation in free convection flow. The viscous dissipation effects on unsteady free convective flow over a vertical porous plate was then investigated by Soundalgekar (1972). Vajravelu and Hadjinicolaou (1993) then studied the viscous dissipation effects on a stretching sheet. Chen (2004) and Partha et al. (2005) observed the mixed and MHD free convection heat transfer from a vertical surface and exponentially stretching surface with Ohmic heating and viscous dissipation, respectively. Recently, Yirga and Shankar (2013) considered this topic with thermal radiation and magnetohydrodynamic effects on the stagnation point flow towards a stretching sheet.

Motivated by the above contributions, the purpose of the present study is to investigate the free convection boundary layer flow towards a horizontal circular cylinder in a nanofluid by including the viscous dissipation effect. The governing partial differential equations were solved numerically and the variation of pertinent physical parameters were analyzed and discussed with the aid of tables and profiles.

Mathematical Formulation

Consider a horizontal circular cylinder of radius a, which is heated to a constant temperature T_w embedded in a nanofluid with ambient temperature T_∞ as shown in Figure 1. The orthogonal coordinates of $\overline{x}$ and $\overline{y}$ is measured along the cylinder surface, starting with the lower stagnation point $\overline{x} = 0$, and normal to it, respectively. Under the assumptions that the boundary layer approximations is valid, the dimensional governing equations of steady free convection boundary layer flow are (Khan & Pop 2010; Salleh & Nazar 2010):

$$\frac{\partial \overline{u}}{\partial \overline{x}} + \frac{\partial \overline{v}}{\partial \overline{y}} = 0, \tag{1}$$

$$\overline{u}\frac{\partial \overline{u}}{\partial \overline{x}} + \overline{v}\frac{\partial \overline{u}}{\partial \overline{y}} = \nu\frac{\partial^2 \overline{u}}{\partial \overline{y}^2} + g\beta(T - T_\infty)\sin\frac{\overline{x}}{a}, \tag{2}$$

$$\overline{u}\frac{\partial T}{\partial \overline{x}} + \overline{v}\frac{\partial T}{\partial \overline{y}} = \alpha\frac{\partial^2 T}{\partial \overline{y}^2} + \tau\left[D_B\frac{\partial C}{\partial \overline{y}}\frac{\partial T}{\partial \overline{y}} + \frac{D_T}{T_\infty}\left(\frac{\partial T}{\partial \overline{y}}\right)^2\right] + \frac{\mu}{\rho C_p}\left(\frac{\partial \overline{u}}{\partial \overline{y}}\right)^2, \tag{3}$$

$$\overline{u}\frac{\partial C}{\partial \overline{x}} + \overline{v}\frac{\partial C}{\partial \overline{y}} = D_B\frac{\partial^2 C}{\partial \overline{y}^2} + \frac{D_T}{T_\infty}\frac{\partial^2 T}{\partial \overline{y}^2}, \tag{4}$$

subject to the boundary conditions

$$\begin{aligned}&\overline{u}(\overline{x},0) = \overline{v}(\overline{x},0) = 0, T(\overline{x},0) = T_w, C(\overline{x},0) = C_w,\\ &\overline{u}(\overline{x},\infty) \to 0,\ T(\overline{x},\infty) \to T_\infty, C(\overline{x},\infty) \to C_\infty,\end{aligned} \tag{5}$$

where $\overline{u}$ and $\overline{v}$ are the velocity components along the $\overline{x}$ and $\overline{y}$ axes, respectively; μ is the dynamic viscosity; ν is the kinematic viscosity; g is the gravity acceleration; β is the thermal expansion; T *is* local temperature; ρ is the fluid density; and C_p is the specific heat capacity at a constant pressure. Furthermore, C is the nanoparticle volume fraction, C_w is the nanoparticle volume fraction C at the surface and C_∞ is the ambient nanoparticle volume fraction C.

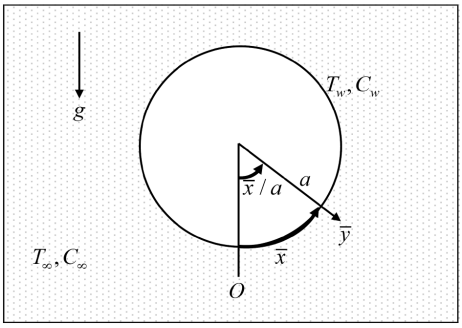

FIGURE 1. Physical model of the coordinate system

Next, it introduced the governing non-dimensional variables:

$$\begin{aligned}x = \frac{\overline{x}}{a}, \quad y = Gr^{1/4}\frac{\overline{y}}{a}, \quad u = \frac{a}{\nu}Gr^{-1/2}\overline{u}, v = \frac{a}{\nu}Gr^{-1/4}\overline{v},\\ \theta(\eta) = \frac{T - T_\infty}{T_w - T_\infty}, \quad \phi(\eta) = \frac{C - C_\infty}{C_w - C_\infty}.\end{aligned} \tag{6}$$

where θ and ϕ are the rescaled dimensionless temperature and nanoparticle volume fraction of the fluid and $Gr = \frac{g\beta(T_w - T_\infty)a^3}{\nu^2}$ is the Grashof number. Using (6), (1)-(4) becomes:

$$\frac{\partial u}{\partial x} + \frac{\partial v}{\partial y} = 0, \tag{7}$$

$$u\frac{\partial u}{\partial x} + v\frac{\partial u}{\partial y} = \frac{\partial^2 u}{\partial y^2} + \theta\sin x, \tag{8}$$

$$u\frac{\partial \theta}{\partial x} + v\frac{\partial \theta}{\partial y} = \frac{\alpha}{\nu}\frac{\partial^2 \theta}{\partial y^2} + \frac{\tau D_B(C_w - C_\infty)}{\nu}\frac{\partial \phi}{\partial y}\frac{\partial \theta}{\partial y} + \frac{\tau D_T(T_w - T_\infty)}{T_\infty \nu}\left(\frac{\partial \theta}{\partial y}\right)^2 + \frac{\nu^2 Gr}{a^2 C_p(T_w - T_\infty)}\left(\frac{\partial u}{\partial y}\right)^2, \tag{9}$$

$$u\frac{\partial \phi}{\partial x}+v\frac{\partial \phi}{\partial y}=\frac{D_B}{\nu}\frac{\partial^2 \phi}{\partial y^2}+\frac{D_T\left(T_w-T_\infty\right)}{T_\infty \nu\left(C_w-C_\infty\right)}\frac{\partial^2 \theta}{\partial y^2}, \quad (10)$$

subject to the boundary conditions:

$$u(x,0)=0,\ v(x,0)=0,\ \theta(x,0)=1,\ \phi(x,0)=1,$$
$$u(x,\infty)\to 0, \theta(x,\infty)\to 0,\ \ \phi(x,\infty)\to 0. \quad (11)$$

In order to solve (7) to (10), the following functions were introduced:

$$\psi = xf(x,y)\ \ \theta=\theta(x,y),\ \phi=\phi(x,y), \quad (12)$$

where ψ is the stream function defined as $u=\frac{\partial \psi}{\partial y}$ and $v=-\frac{\partial \psi}{\partial x}$ which identically satisfies (7). Substitute (12) into (7)-(10), the following partial differential equations were obtained:

$$\frac{\partial^3 f}{\partial y^3}+f\frac{\partial^2 f}{\partial y^2}-\left(\frac{\partial f}{\partial y}\right)^2+\theta=x\left(\frac{\partial f}{\partial y}\frac{\partial^2 f}{\partial x\partial y}-\frac{\partial f}{\partial x}\frac{\partial^2 f}{\partial y^2}\right), \quad (13)$$

$$\frac{1}{\Pr}\frac{\partial^2 \theta}{\partial y^2}+f\frac{\partial \theta}{\partial y}+N_b\frac{\partial \phi}{\partial y}\frac{\partial \theta}{\partial y}+N_t\left(\frac{\partial \theta}{\partial y}\right)^2=$$
$$x\left(\frac{\partial f}{\partial y}\frac{\partial \theta}{\partial x}-\frac{\partial f}{\partial x}\frac{\partial \theta}{\partial y}-xEc\left(\frac{\partial^2 f}{\partial y^2}\right)^2\right), \quad (14)$$

$$\frac{\partial^2 \phi}{\partial y^2}+\frac{N_t}{N_b}\frac{\partial^2 \theta}{\partial y^2}+Lef\frac{\partial \phi}{\partial y}=xLe\left(\frac{\partial f}{\partial y}\frac{\partial \phi}{\partial x}-\frac{\partial f}{\partial x}\frac{\partial \phi}{\partial y}\right), \quad (15)$$

where $\Pr=\frac{\nu}{\alpha}$ is the Prandtl number; $N_b=\frac{\tau D_B(C_w-C_\infty)}{\nu}$ is the Brownian motion parameter, $N_t=\frac{\tau D_T(T_w-T_\infty)}{T_\infty \nu}$ is the thermophoresis motion parameter, $Ec=\frac{\nu^2 Gr}{a^2 C_p\left(T_w-T_\infty\right)}$ is an Eckert number; and $Le=\frac{\nu}{D_B}$ is the Lewis number. The boundary conditions (11) becomes:

$$f(x,0)=0,\ \ \frac{\partial f}{\partial y}(x,0)=0,\ \ \theta(x,0)=1,\ \ \phi(x,0)=1,$$
$$\frac{\partial f}{\partial y}(x,\infty)\to 0,\ \ \theta(x,\infty)\to 0,\ \ \phi(x,\infty)\to 0. \quad (16)$$

The physical quantities of interest are the skin friction coefficient C_f, the local Nusselt number Nu_x and the Sherwood number Sh_x which are given by Molla et al. (2006)

$$C_f=\frac{\tau_w}{\rho u_\infty^2},\ Nu_x=\frac{aq_w}{k(T_w-T_\infty)},\ Sh_x=\frac{aj_w}{D_B(C_w-C_\infty)}, \quad (17)$$

where ρ is the fluid density. The surface shear stress τ_w the surface heat flux q_w and the surface mass flux j_w are given by:

$$\tau_w=\mu\left(\frac{\partial \overline{u}}{\partial \overline{y}}\right)_{\overline{y}=0},\ q_w=-k\left(\frac{\partial T}{\partial \overline{y}}\right)_{\overline{y}=0},\ j_w=-D_B\left(\frac{\partial C}{\partial \overline{y}}\right)_{\overline{y}=0}, \quad (18)$$

with $\mu=\rho\nu$ and k being the dynamic viscosity and the thermal conductivity, respectively.

Using variables (6) and (12) give:

$$C_f Gr^{1/4}=\left(x\frac{\partial^2 f}{\partial y^2}\right)_{\overline{y}=0},\ Nu_x Gr^{-1/4}=-\left(\frac{\partial \theta}{\partial y}\right)_{\overline{y}=0}$$
$$\text{and}\ \ Sh_x Gr^{-1/4}=-\left(\frac{\partial \phi}{\partial y}\right)_{\overline{y}=0} \quad (19)$$

Furthermore, the velocity profiles and temperature distributions can be obtained from the following relations:

$$u=f'(x,y),\ \ \theta=\theta(x,y), \quad (20)$$

Numerical Method

The partial differential equations (13) to (15) subject to boundary conditions (16) are solved numerically using the Keller-box method, which is an implicit finite difference method in conjunction with Newton's method for linearization. This made it suitable to solve parabolic partial differential equations. The previous studies which used Keller-box method in solving the boundary layer problems including Ishak et al. (2007, 2006), Nazar et al. (2004, 2003) and Salleh et al. (2011, 2009).

Results and Discussion

Equations (13)-(15) subject to the boundary conditions (16) were solved numerically using the Keller-box method with five parameters considered, namely the Prandtl number Pr the Brownian motion parameter N_b, thermophoresis parameter N_t, Lewis number Le and the Eckert number Ec. The step size $\Delta y = 0.02$, $\Delta x = 0.005$ and boundary layer thickness $y_\infty = 8$ and $x_\infty = \pi$ are used in obtaining the numerical results. Furthermore, the value of Pr is set to be Pr = 7 which represents water that usually acts as the base fluid for the nanofluid. Tables 1 and 2 show the comparison values of $Nu_x Gr^{-1/4}$ and $CfGr^{1/4}$ with previous results for various values of x, respectively. It has been found that they are in good agreement. It was concluded that this method works efficiently hence, the results presented here are confidently accurate.

Figure 2 illustrated the variations of reduced skin friction coefficient $C_f Gr^{1/4}$ against x for various values of N_b and N_t. From this figure, it was concluded that the effects of N_b and N_t are more pronounced as x increases to the middle of cylinder. It is clearly shown that the increase of N_b and N_t results to the increase of $C_f Gr^{1/4}$.

TABLE 1. Comparison values of $Nu_x Gr^{-1/4}$ with previous published results for various values of x when Pr = 1 and $N_b = N_t = Le = Ec = 0$

x	Merkin (1976)	Nazar et al. (2002)	Molla et al. (2006)	Salleh and Nazar (2010)	Azim (2014)	Present
0	0.4214	0.4214	0.4214	0.4214	0.4216	0.4214
π/6	0.4161	0.4161	0.4161	0.4162	0.4163	0.4163
π/3	0.4007	0.4005	0.4005	0.4006	0.4006	0.4008
π/2	0.3745	0.3741	0.3740	0.3744	0.3742	0.3744
2π/3	0.3364	0.3355	0.3355	0.3360	0.3356	0.3364
5π/6	0.2825	0.2811	0.2812	0.2817	0.2811	0.2824
π	0.1945	0.1916	0.1917	0.1939	0.1912	0.1939

TABLE 2. Comparison values of $C_f Gr^{1/4}$ with previous published results for various values of x when Pr = 1 and $N_b = N_t = Le = Ec = 0$

x	Merkin (1976)	Nazar et al. (2002)	Molla et al. (2006)	Azim (2014)	Present
0	0.0000	0.0000	0.0000	0.0000	0.0000
π/6	0.4151	0.4148	0.4145	0.4139	0.4121
π/3	0.7558	0.7542	0.7539	0.7528	0.7538
π/2	0.9579	0.9545	0.9541	0.9526	0.9563
2π/3	0.9756	0.9698	0.9696	0.9678	0.9743
5π/6	0.7822	0.7740	0.7739	0.7718	0.7813
π	0.3391	0.3265	0.3264	0.3239	0.3371

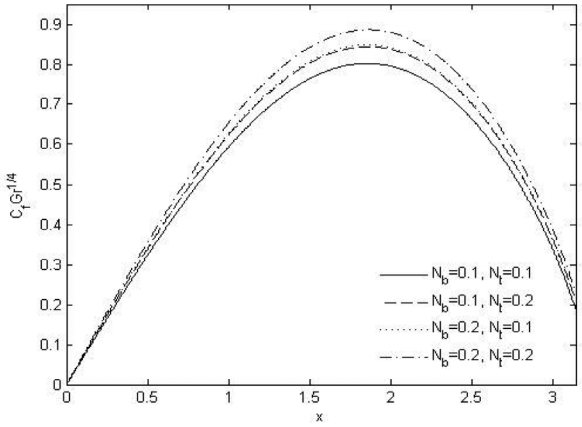

FIGURE 2. Variation of reduced skin friction coefficient $C_f Gr^{1/4}$ against x for various values of N_b and N_t

Next, Figures 3 and 4 show the variations of the reduced Nusselt number $Nu_x Gr^{-1/4}$ and Sherwood number $Sh_x Gr^{-1/4}$ for various values of N_b and N_t, respectively. In Figure 3, it was found that $Nu_x Gr^{-1/4}$ decreases as N_b and N_t increase. It was found that, the higher values of N_b and N_t subsequently results to higher volume of nanoparticles migrating away from the vicinity of the wall and thus reduces the value of the Nusselt number. In Figure 4, the trend is contrary with Figure 3 where an increase of N_b and N_t results to the increase of $Sh_x Gr^{-1/4}$. Furthermore, from both figures, it was suggested that as the flow past the cylinder, the influence of N_b and N_t getting lesser than the stagnation region ($x \approx 0$).

Figures 5 and 6 display the velocity and temperature profiles for various values of N_b and N_t, respectively. It was found that the increase of N_b and N_t results to the increase in velocity and temperature distribution. This phenomenon is realistic where the presence of nanoparticles in nanofluid will enhance the heat transfer characteristics as well as thermal conductivity. Furthermore, it was worth to state that N_b and N_t do not influence much in the changes of boundary layer thicknesses.

In order to understand the behaviour of Lewis number Le and Eckert number Ec in this convective boundary layer flow, Figures 7 to 11 were plotted. Figures 7 to 9 show the variations of $C_f Gr^{1/4}$, $Nu_x Gr^{-1/4}$ and $Sh_x Gr^{-1/4}$ with various

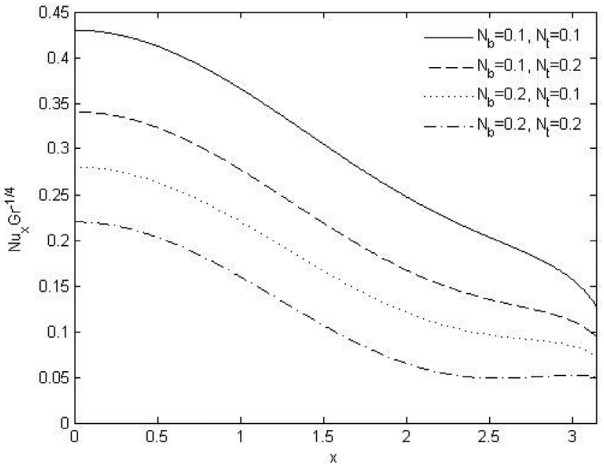

FIGURE 3. Variation of reduced Nusselt number $Nu_x Gr^{-1/4}$ against x for various values of N_b and N_t

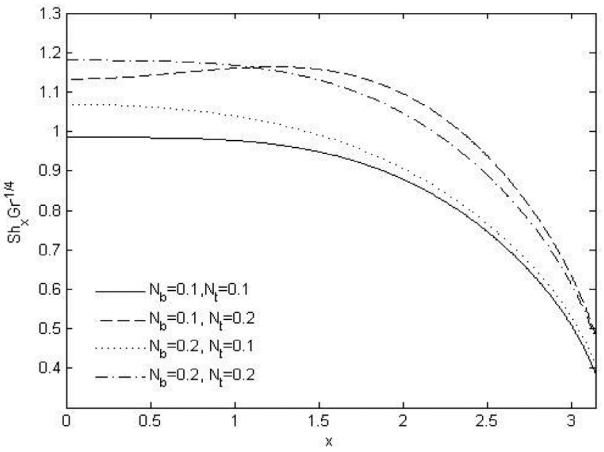

FIGURE 4. Variation of reduced Sherwood number $Sh_x Gr^{-1/4}$ against x for various values of N_b and N_t

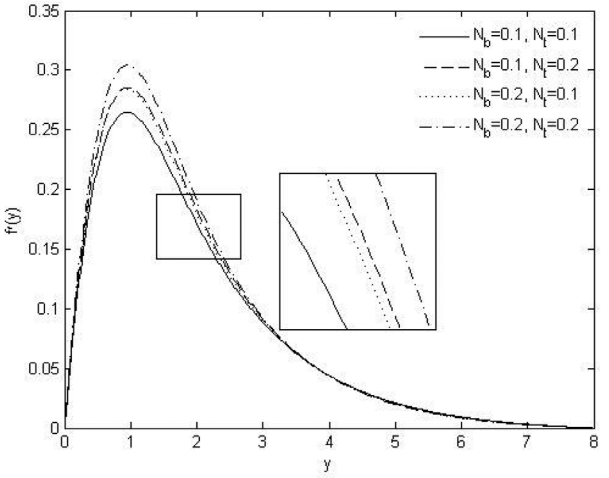

FIGURE 5. Velocity profiles $f'(y)$ against y for various values of N_b and N_t

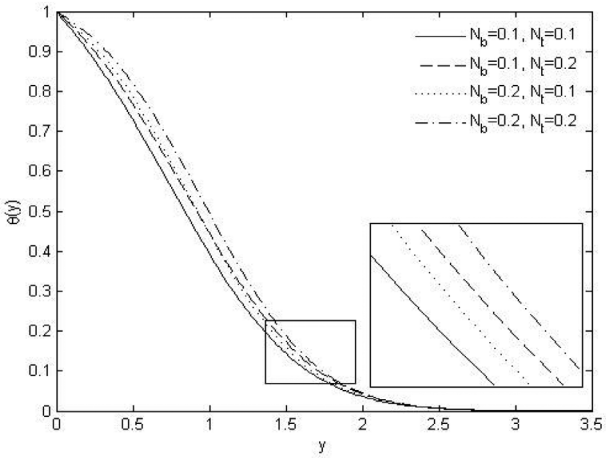

FIGURE 6. Temperature profiles $\theta(y)$ against y for various values of N_b and N_t

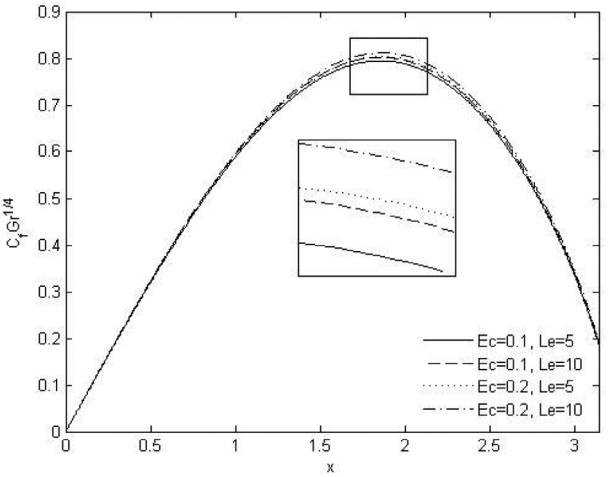

FIGURE 7. Variation of reduced skin friction coefficient $C_f Gr^{1/4}$ against x for various values of Ec and Le

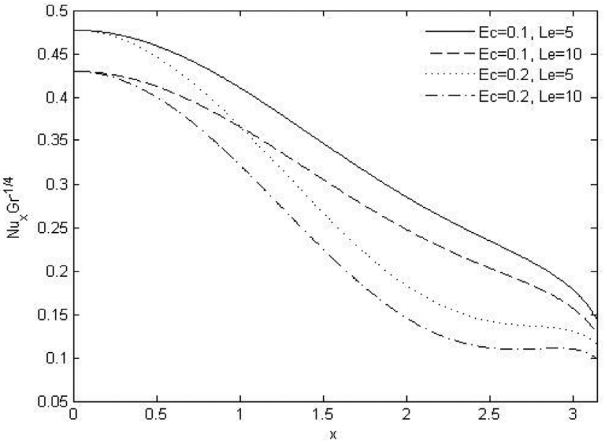

FIGURE 8. Variation of reduced Nusselt number $Nu_x Gr^{-1/4}$ against x for various values of Ec and Le

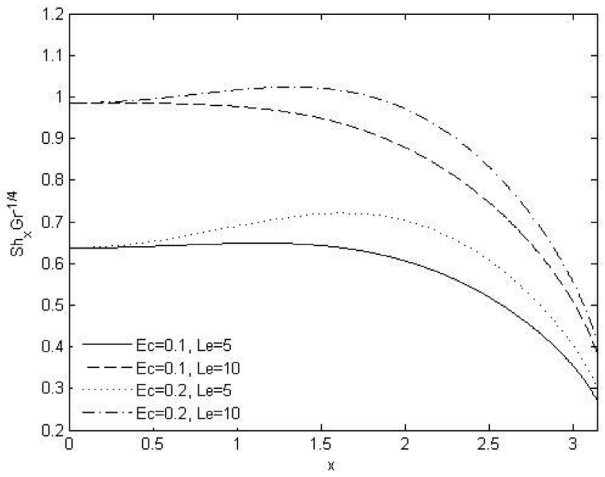

FIGURE 9. Variation of reduced Sherwood number $Sh_x Gr^{-1/4}$ against x for various values of Ec and Le

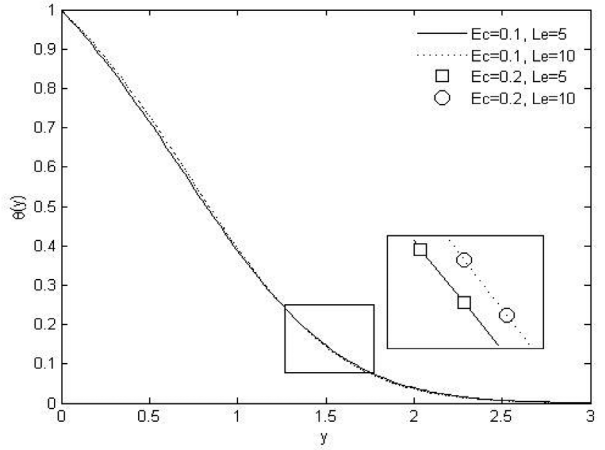

FIGURE 10. Temperature profiles $\theta(y)$ against y for various values of Ec and Le

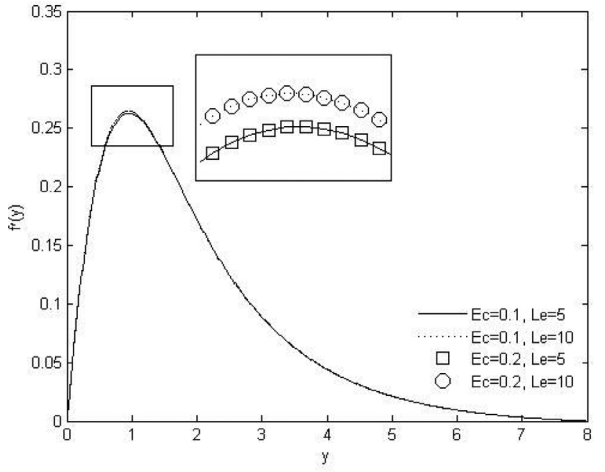

FIGURE 11. Velocity profiles $f'(y)$ against y for various values of Ec and Le

values of Ec and Le. From Figure 7, it was found that the value of $C_f Gr^{1/4}$ is unique for all values of Ec and Le at the early stage. From this figure, it was understand that Ec and Le gave a small influence on $C_f Gr^{1/4}$. The effects of Ec and Le are significance as x increase to the middle of cylinder then converge back at the end of the cylinder ($x = \pi$). In Figures 8 and 9, it is notice that the effect of Ec is negligible at the lower stagnation region ($x = 0$). As x increases, $Nu_x Gr^{-1/4}$ decreases for all set of parameter Ec and Le. Furthermore, the increase of both parameters Ec and Le may results to the decrease of $Nu_x Gr^{-1/4}$ while $Sh_x Gr^{-1/4}$ increase. This is due to the mass diffusivity is more dominant than thermal diffusivity, where the transient mass response is quicker than the transient thermal response to the change of Le and temperature.

Lastly, Figures 10 and 11 display the temperature and velocity profiles for various values of Ec and Le, respectively. It was found that the effect of Le is very small while Ec gives no effects on the temperature and velocity distributions as well as the boundary layer thicknesses. The increase of Le results to the slightly increase in thermal boundary layer thickness and velocity distribution.

CONCLUSION

In this paper, we have numerically studied the problem of free convection boundary layer flow on a horizontal circular cylinder in a nanofluid with viscous dissipation and constant wall temperature. It was concluded that the increase of the Brownian motion parameter, thermophoresis parameter, Lewis number and Eckert number results in the increase of skin friction coefficient and Sherwood number while Nusselt number decreases. This is due to the increase of nanofluid parameters which increase the volume of nanoparticles migrating away from the vicinity of the wall and thus reduce the value of the Nusselt number. Furthermore, it was found that the Eckert number which represents the viscous dissipation effect gives no effects on the temperature and velocity profiles.

ACKNOWLEDGEMENTS

The authors gratefully acknowledge the financial support received from the Universiti Malaysia Pahang (RDU150101& RDU140111).

REFERENCES

Anwar, I., Qasim, A.R., Ismail, Z., Salleh, M.Z. & Shafie, S. 2013. Chemical reaction and uniform heat generation/absorption effects on MHD stagnation-point flow of a nanofluid over a porous sheet. *World Applied Sciences Journal* 24(10): 1390.

Arifin, N.M., Nazar, R. & Pop, I. 2011. Viscous flow due to a permeable stretching/shrinking sheet in a nanofluid. *Sains Malaysiana* 40(12): 1359-1367.

Azim, N.H.M.A. 2014. Effects of viscous dissipation and heat generation on MHD conjugate free convection flow from an isothermal horizontal circular cylinder. *SOP Transactions on Applied Physics* 1(3): 1-11.

Bachok, N., Ishak, A. & Pop, I. 2010. Boundary-layer flow of nanofluids over a moving surface in a flowing fluid. *International Journal of Thermal Sciences* 49(9): 1663-1668.

Blasius, H. 1908. Grenzschichten in Flssigkeiten mit kleiner Reibung. *Zeitschrift f¨urangewandte Mathematik und Physik* 56: 1-37.

Chen, C.H. 2004. Combined heat and mass transfer in MHD free convection from a vertical surface with Ohmic heating and viscous dissipation. *International Journal of Engineering Science* 42(7): 699-713.

Fr¨ossling, N. 1958. Calculating by series expansion of the heat transfer in laminar, constant property boundary layers at non isothermal surfaces. *Archiv f¨or Fysik* 14: 143-151.

Gebhart, B. 1962. Effects of viscous dissipation in natural convection. *Journal of Fluid Mechanics* 14(02): 225-232.

Ishak, A., Nazar, R., Amin, N., Filip, D. & Pop, I. 2007. Mixed convection of the stagnation-point flow towards a stretching vertical permeable sheet. *Malaysian Journal of Mathematical Sciences* 2: 217-226.

Ishak, A., Nazar, R. & Pop, I. 2006. Mixed convection boundary layers in the stagnation-point flow toward a stretching vertical sheet. *Meccanica* 41(5): 509-518.

Kakaç, S. & Pramuanjaroenkij, A. 2009. Review of convective heat transfer enhancement with nanofluids. *International Journal of Heat and Mass Transfer* 52(13-14): 3187-3196.

Khan, W.A. & Pop, I. 2010. Boundary-layer flow of a nanofluid past a stretching sheet. *International Journal of Heat and Mass Transfer* 53(11-12): 2477-2483.

Merkin, J.H. & Pop, I. 1988. A note on the free convection boundary layer on a horizontal circular cylinder with constant heat flux. *Wärme - und Stoffübertragung* 22(1-2): 79-81.

Merkin, J.H. 1977. Mixed convection from a horizontal circular cylinder. *International Journal of Heat and Mass Transfer* 20(1): 73-77.

Merkin, J.H. 1976. Free convection boundary layer on an isothermal horizontal cylinder. *ASME/AIChe Heat Transfer Conference*, St. Louis, USA.

Molla, M.M., Hossain, M.A. & Paul, M.C. 2006. Natural convection flow from an isothermal horizontal circular cylinder in presence of heat generation. *International Journal of Engineering Science* 44(13-14): 949-958.

Nazar, R., Jaradat, M., Arifin, N. & Pop, I. 2011. Stagnation-point flow past a shrinking sheet in a nanofluid. *Central European Journal of Physics* 9(5): 1195-1202.

Nazar, R., Amin, N., Filip, D. & Pop, I. 2004. Stagnation point flow of a micropolar fluid towards a stretching sheet. *International Journal of Non-Linear Mechanics* 39(7): 1227-1235.

Nazar, R., Amin, N. & Pop, I. 2003. Mixed convection boundary-layer flow from a horizontal circular cylinder in micropolar fluids: Case of constant wall temperature. *International Journal of Numerical Methods for Heat & Fluid Flow* 13(1): 86-109.

Nazar, R., Amin, N. & Pop, I. 2002. Free convection boundary layer on an isothermal horizontal circular cylinder in a micropolar fluid. *Proceedings of Tweifth Int Heat Transfer Conference*. Paris, Elsevier. 2: 525-530.

Partha, M.K., Murthy, P. & Rajasekhar, G.P. 2005. Effect of viscous dissipation on the mixed convection heat transfer from an exponentially stretching surface. *Heat and Mass Transfer* 41(4): 360-366.

Rosca, A.V., Rosca, N.C. & Pop, I. 2014. Note on dual solutions for the mixed convection boundary layer flow close to the lower stagnation point of a horizontal circular cylinder: Case of constant surface heat flux. *Sains Malaysiana* 43(8): 1239-1247.

Roşca, N.C. & Pop, I. 2014. Unsteady boundary layer flow of a nanofluid past a moving surface in an external uniform free stream using Buongiorno's model. *Computers & Fluids* 95(0): 49-55.

Salleh, M.Z., Nazar, R. & Pop, I. 2011. Numerical solutions of forced convection boundary layer flow on a horizontal circular cylinder with Newtonian heating. *Malaysian Journal of Mathematical Sciences* 5(2): 161-184.

Salleh, M.Z. & Nazar, R. 2010. Free convection boundary layer flow over a horizontal circular cylinder with Newtonian heating. *Sains Malaysiana* 39(4): 671-676.

Salleh, M.Z., Nazar, R. & Pop, I. 2009. Forced convection boundary layer flow at a forward stagnation point with Newtonian heating. *Chemical Engineering Communications* 196: 987-996.

Sarif, N.M., Salleh, M.Z., Tahar, R.M. & Nazar, R. 2014. Numerical solution of the free convection boundary layer flow over a horizontal circular cylinder with convective boundary conditions. *AIP Conference Proceedings* 1602: 179-185.

Singh, G. & Makinde, O.D. 2014. Axisymmetric slip flow on a vertical cylinder with heat transfer. *Sains Malaysiana* 43(3): 483-489.

Soundalgekar, V.M. 1972. Viscous dissipation effects on unsteady free convective flow past an infinite, vertical porous plate with constant suction. *International Journal of Heat and Mass Transfer* 15(6): 1253-1261.

Tahavvor, A.R. & Yaghoubi, M. 2010. Experimental and numerical study of frost formation by natural convection over a cold horizontal circular cylinder. *International Journal of Refrigeration* 33(7): 1444-1458.

Tham, L., Nazar, R. & Pop, I. 2014. Mixed convection flow from a horizontal circular cylinder embedded in a porous medium filled by a nanofluid: Buongiorno-Darcy model. *International Journal of Thermal Sciences* 84: 21-33.

Tham, L. & Nazar, R. 2012. Mixed convection flow about a solid sphere embedded in a porous medium filled with a nanofluid. *Sains Malaysiana* 41(12): 1643-1649.

Tiwari, R. & Das, M. 2007. Heat transfer augmentation in a two-sided lid-driven differentially heated square cavity utilizing nanofluids. *Int. J. Heat Mass Transf.* 50: 2002-2018.

Vajravelu, K. & Hadjinicolaou, A. 1993. Heat transfer in a viscous fluid over a stretching sheet with viscous dissipation and internal heat generation. *International Communications in Heat and Mass Transfer* 20(3): 417-430.

Wong, K.V. & De Leon, O. 2010. Applications of nanofluids: Current and future. *Advances in Mechanical Engineering* 2: 519659.

Yacob, N.A., Ishak, A., Pop, I. & Vajravelu, K. 2011. Boundary layer flow past a stretching/shrinking surface beneath an external uniform shear flow with a convective surface boundary condition in a nanofluid. *Nanoscale Research Letters* 6(1): 1-7.

Yirga, Y. & Shankar, B. 2013. Effects of thermal radiation and viscous dissipation on magnetohydrodynamic stagnation point flow and heat transfer of nanofluid towards a stretching sheet. *Journal of Nanofluids* 2(4): 283-291.

Yusoff, N.H.M., Uddin, M.J. & Ismail, A.I.M. 2014. Combined similarity-numerical solutions of MHD boundary layer slip flow of non-Newtonian power-law nanofluids over a radiating moving plate. *Sains Malaysiana* 43(1): 151-159.

Muhammad Khairul Anuar Mohamed, Nor Aida Zuraimi Md Noar & Mohd Zuki Salleh*
Applied & Industrial Mathematics Research Group
Faculty of Industrial Sciences and Technology
Universiti Malaysia Pahang
26300 Kuantan, Pahang Darul Makmur
Malaysia

Anuar Ishak
School of Mathematical Sciences
Faculty of Science and Technology
Universiti Kebangsaan Malaysia
43600 Bangi, Selangor Darul Ehsan
Malaysia

*Corresponding author; email: zukikuj@yahoo.com

Received: 10 April 2015
Accepted: 2 July 2015